How to cite: *Angew. Chem. Int. Ed.* **2023**, *62*, e202308339
doi.org/10.1002/anie.202308339

Polymerization

Exploiting the Use of the Decarboxylative S-Alkylation Reaction to Produce Self-Blowing, Recyclable Polycarbonate Foams

*Tansu Abbasoglu, Diego Ciardi, Francois Tournilhac, Lourdes Irusta, and Haritz Sardon**

Abstract: Polymeric foams are widely used in many industrial applications due to their light weight and superior thermal, mechanical, and optical properties. Currently, increasing research efforts is being directed towards the development of greener foam formulations that circumvent the use of isocyanates/blowing agents that are commonly used in the production of foam materials. Here, a straightforward, one-pot method is presented to prepare self-blown polycarbonate (PC) foams by exploiting the (decarboxylative) S-alkylation reaction for in situ generation of the blowing agent (CO_2). The concomitant formation of a reactive alcohol intermediate promotes a cascade ring-opening polymerization of the cyclic carbonates to yield a cross-linked polymer network. It is shown that these hydroxyl-functionalized polycarbonate-based foams can be easily recycled into films through thermal compression molding. Furthermore, it is demonstrated that complete hydrolytic degradation of the foams is possible, thus offering the potential for zero-waste materials. This straightforward and versatile process broadens the scope of isocyanate-free, self-foaming materials, opening a new pathway for next-generation environmentally friendly foams.

Introduction

Polymeric foams represent a large class of cellular solids that are used in a diverse range of applications such as thermal insulation materials, packaging materials, automotive materials, and construction materials.[1] Polymer foams have long been of commercial interest due to the advantages of the two-phase system in which gas-filled voids (bubbles) are surrounded by a solid polymer matrix.[2] These porous materials offer unique structural and mechanical properties including lightness, thermal insulation, energy absorption, and mechanical strength per weight unit as compared to their single-phase solid counterparts.[2,3] Furthermore, foam properties can be tuned on demand depending on their chemical structure and morphology, thus allowing for tailored foams for specific applications.[4]

Currently, it is possible to create foam structures using a wide range of polymeric materials.[5] However, the foam industry is dominated by polyurethane (PU) foams, which account for approximately 50 % of the global annual foam production.[6] The primary driver behind the success of PU foams is their self-foaming (or self-blowing) ability. PU foams are commonly produced from polyol/polyisocyanate reactive formulations incorporating a small amount of water (Scheme 1a).[7] The construction of the PU matrix is realized concurrently with the partial hydrolysis of isocyanates that enables in situ formation of carbon dioxide (CO_2) as a blowing agent, facilitating the self-blowing of PU foams. In addition, the primary amine thereby generated participates in the network formation by establishing urea bonds.[8] Despite their desirable properties, PU foams have raised concerns regarding their adverse impacts on human health and the environment. Hence, this chemistry faces increasingly strict regulations every year aimed at limiting the use

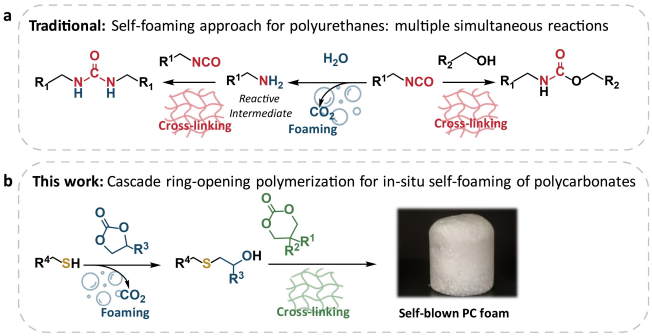

Scheme 1. General comparison of the self-foaming approaches for PUs and PCs, highlighting the similarities between the gelation and foaming processes. (a) Overview of the traditional self-foaming method for PUs to execute multiple, simultaneous reactions. (b) General description of a decarboxylative cascade ring-opening polymerization for the preparation of self-blown PC foams facilitated by an in situ formed reactive β-hydroxythioether intermediate upon the S-alkylation by the cyclic carbonate.

[*] T. Abbasoglu, Prof. Dr. L. Irusta, Prof. Dr. H. Sardon
POLYMAT, University of the Basque Country UPV/EHU,
Joxe Mari Korta Center, Avda. Tolosa 72, 20018 Donostia-San Sebastian (Spain)
E-mail: haritz.sardon@ehu.eus
D. Ciardi, F. Tournilhac
Molecular, Macromolecular Chemistry,and Materials,
CNRS, ESPCI-Paris, PSL Research University
10 rue Vauquelin, 75005 Paris (France)

of toxic isocyanates in PU foam production. Therefore, intense scientific efforts are headed towards generation of alternative self-foaming systems that mimic conventional PU foaming processes without relying on isocyanate hydrolysis.

In the pioneering work of Caillol et al., non-isocyanate polyurethane foams were obtained through in situ release of H_2 delivered by a hydroxysiloxane blowing agent.[9] Along these lines, Detrembleur et al. relied on the (decarboxylative) S-alkylation which involves the nucleophilic addition of thiols to five-membered cyclic carbonates (5CCs) leading to in situ released CO_2 on a transition towards self-blowing isocyanate-free polyurethanes.[10] We hypothesize that by tailored use of the (decarboxylative) S-alkylation, foams from other polymer families could also be prepared. Thus, we envisioned that other industrially relevant eco-friendly alternative of polymer foam precursors such as polycarbonates (PCs), which hold great potential for sustainability, could be designed using the (decarboxylative) S-alkylation.

Among the different polycarbonates, aliphatic polycarbonates (APCs) have been historically investigated due to their susceptibility to hydrolysis.[11,12] Moreover, APCs can be obtained from a range of different sustainable sources, including natural and renewable sources, as well as by chemical decomposition. The paradoxical nature of APCs reveal their circular end-of-life possibilities that offer a solution to the accumulation of plastic waste, which is a major issue of modern society.[13] Consequently, in recent decades, this cleanness/greenness/lack of toxicity has stimulated considerable research efforts in the design and potential applicability of such materials in diverse field, including medical and pharmaceutical applications as well as energy storage.[13,14]

Despite the promise of APCs, the lack of convenient synthetic methods for their foaming is an obstacle for their exploitation in industry. The foaming of PCs with a primary focus on aromatic polycarbonates like Lexan has been extensively studied because of their good mechanical properties; however, to our knowledge, expanded polycarbonates are limited to thermoplastic foam systems that can be fabricated via conventional techniques of foam extrusion, molded bead, and injection molding using a physical blowing agent, e.g., CO_2 and n-pentane.[15] Externally-blown foams cannot mimic the cell uniformity and properties of self-blown foams, while the addition of external blowing agents increases the cost and complexity of the industrial production process.[3]

On this backdrop, we suggest a fundamentally new approach where the thiol/5CC reaction provides in situ generated blowing agent, as well as the β-hydroxythioether that initiates the ring-opening of a 6CC monomer, ultimately leading to the self-blown PC foam (Scheme 1b). We have taken advantage of the negligible reactivity of 6-membered cyclic carbonates (6CCs) towards thiols whereas they are more prone to alcoholysis in contrast to 5CCs. These features were exploited and here, we report the first proof-of-concept study that demonstrates the preparation of self-blowing PC foams by merging the two reactions required to form a homogeneous cellular structure into a single-step process. We also showcase the potential of these foams to be recycled by both mechanical and chemical recycling processes.

Results and Discussion

Concept and Formulation Development

The primary challenge in the formation and subsequent stability of foams is the need to tune the viscosity and cross-linking degree so as to ensure successful gas entrapment and foam rise whilst preventing structural collapse.[16] In particular, self-blowing processes are regulated by the kinetics of two processes, (i) the gelation or cross-linking and (ii) the generation of blowing agent (CO_2). These two processes need to proceed in parallel to avoid poor cellular structure. Therefore, merging the two processes into a single step is key to making the production of self-blown PCs feasible.

In order to understand the reactivity of cyclic carbonates with nucleophiles (e.g., thiols and alcohols) and how to apply this to foam synthesis, we first investigated the organobase-catalyzed addition of a diol (triethylene glycol) and a dithiol (3,6-dioxa-1,8-octanedithiol) to a model compounds 5CC (ethylene carbonate, abbreviated hereafter as C5) and 6CC (5,5-dimethyl-trimethylene carbonate, abbreviated as C6) (Figure 1). These reactions were realized using equimolar ratios of the reactive groups at 70 °C with DBU (5 mol %) as a catalyst. DBU was added as it was reported to be necessary to promote the CO_2 formation upon decarboxylative S-alkylation.[10] The reactions were monitored by ^{1}H NMR (Supporting Information, Figures S1–S4).

Figure 1a shows that in the case of C6, the thiol did not react. In contrast, the alcohol led to the relatively rapid ring opening of C6 to yield oligocarbonate diols (98 % C6 conversion in 1 h). However, the reverse trend was observed

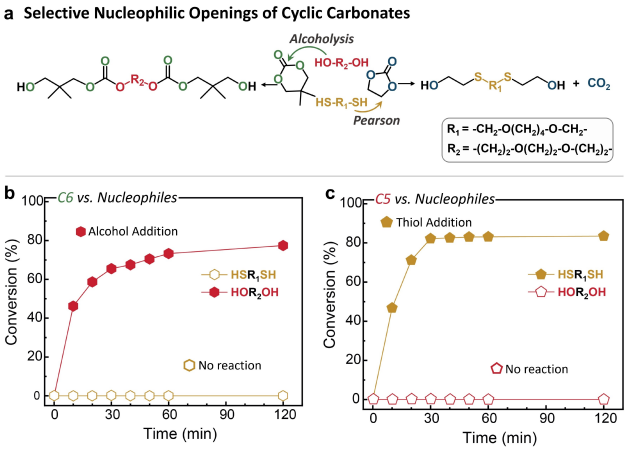

Figure 1. (a) Selective nucleophilic openings of cyclic carbonates with regioselectivity by different nucleophiles. (b) Conversion of C6 and (c) C5 with the reaction time through ring-opening reactions with the dithiol or diol. Conditions: (a) [SH] or [OH]/[C6] = 1 and (b) [SH] or [OH]/[C5] = 1, 5 mol% of DBU vs. the cyclic carbonate. Reactions at 70 °C in anhydrous DMSO.

with the model 6CC; In the case of C5 the thiol provided the expected hydroxythioethers upon decarboxylative S-alkylation, while the ring-opening of C5 with the alcohol was not observed (Figure 1b). Thus, by a judicious choice of nucleophiles, the (chemo)-selective ring-opening of cyclic carbonates could be facilitated. This distinct reactivity is likely due to the interplay between the ring strain and conformational preferences of 5- and 6-membered cyclic carbonates. The sterically hindered conformation of the 6-membered ring, wherein higher ring strain is present, could lead to the restricted accessibility of the larger size of the incoming sulfur atoms. Conversely, the more planar 5-membered ring with the reduced ring strain tends to increase the reactivity towards thiols.

To confirm the feasibility of the proposed one-step methodology to yield cross-linked polycarbonates foams, a tricomponent reaction was conducted, for which the reaction progress was monitored by ATR-IR analysis (Figure S5). We initially hypothesized that the alcohol that would be generated after the (decarboxylative) S-alkylation reaction could subsequently be reacted in a cascade reaction to initiate the gelling reaction, in which case there would be no need for an external alcohol source. Therefore we prepared a formulation containing, the bis(6-membered cyclic carbonate) BC6 (di(trimethylolpropane) carbonate), and the monofunctional 5-membered cyclic carbonate C5 (ethylene carbonate), and the dithiol (3,6-dioxa-1,8-octanedithiol). For [BC6]/[C5]/[SH] = 1/2/2 with DBU (5 mol%), the vibrational frequency of C=O groups around 1800 cm^{-1} disappeared in 2 h at 70 °C, showing the almost total consumption of the cyclic carbonate species. The peaks at 1741 cm^{-1} and 1236 cm^{-1}, ascribed to the stretching vibration of C=O and C–O–C bands, respectively, confirmed the formation of a network bearing linear carbonate linkages. The disappearance of the peak at around 2560 cm^{-1} suggests the consumption of thiol functional groups (SH). The resulting foam was sticky with a lack of rigidity and structural stability (Figure S6). Our starting hypothesis was thus validated, demonstrating the potential formation of a cross-linked network concomitant with the generation of CO_2. However, the foam formation processes must be optimized by the careful selection of the conditions such as temperature, (co)reactant choices, surfactant, and stoichiometric ratios.

Mimicking the Foaming Process of Polyurethanes

While the self-foaming potential of PU formulations relies on the hydrolysis of isocyanates, the decarboxylative S-alkylation with EC unlocks the self-foaming ability in our isocyanate-free PC formulations. In PU foams, water and isocyanate functional groups react to form unstable carbamic acids, which subsequently decompose to give the blowing agent, CO_2, and an amine. The latter reacts in a side reaction with unhydrolyzed isocyanates, leading to the formation of urea bonds. The amount of water determines how much gas (CO_2) is released, which directly governs the morpho-structural properties (i.e., the cells size and distribution, open and/or closed cells).[17] To define an optimal foaming window, we therefore started by changing the molar concentration of ethylene carbonate, which decarboxylates via methylene attack of thiols, mimicking the PU foaming process. To this end, various reactive formulations with different ratios of the BC6, 5 C, and a tetrathiol (such as pentaerythritol tetrakis (3-mercaptopropionate) (PETMP) were prepared (see Figure S7; see also Table 1). All these formulations contained equimolar amounts of 5 C and PETMP. In the first instance, BC6 and C5 were used at a 1/2 stoichiometric ratio. In this case the foam suffered from rapid bubble enlargement due to an early gas breakthrough in the excessively soft polymer matrix. This led to an overly open structurally stable (Figure S7a). On the contrary, lowering the extent of gas formation by changing the ratio of BC6/C5 to 2/1 restricted bubble coalescence and blowing (Figure S7b). Therefore, we fixed the ratio of BC6/C5 to 1/1 (at equimolar ratio), which enables the self-blown PC foams to be good structural stability (Figure S7c). This simple approach therefore allows the formation of in situ CO_2 by the decarboxylation of one of the comonomers, whereby the final foam properties can be tailored on demand by bluadjusting the amount of C5.

To further elucidate these findings, the gelation time (t_{gel}) and complex viscosity (η^*) were measured as a function of time by oscillatory time sweep tests at a fixed strain and frequency of 1 % and 1 Hz, respectively. In this paper, we estimate t_{gel} by assuming that the starting point of the gelation is where the rate of viscosity reaches a maximum (when the second derivative of the curve shows a peak) (see Table S2 in the supplemental material). We observed that the increase in molar concentration of PETMP from 0.125 to 0.5 (as compared to BC6) substantially reduced the

Table 1: Properties and morphological characterization of self-blown.

Entry	[DTMPC]/[PETMPC]/[EC]	[DTMPC]/[PCL]	Additives	Density [g cm^{-3}]	Pore size [mm]	A_h/A_c	$T_{d5\%}$ [°C]	T_g [°C]
1	1/0.125/0.5	–	None	n.d.[a]	n.d.[a]	n.d.[a]	n.d.[a]	n.d.[a]
2	1/0.25/1	–	None	n.d.[a]	n.d.[a]	n.d.[a]	n.d.[a]	n.d.[a]
3	1/0.5/2	–	None	n.d.[a]	n.d.[a]	n.d.[a]	n.d.[a]	n.d.[a]
4	1/0.25/1	1/1	None	0.180 ± 0.005	n.d.[a]	n.d.[a]	115/222[b]	−14
5	1/0.25/1	1/1	Laponite	0.200 ± 0.005	0.70 ± 0.29	10.6	121	−15
6	1/0.25/1	1/1	Di-TMP	0.278 ± 0.007	0.98 ± 0.37	9.1	120	−16

[a] Not determined due to sample morphology. [b] Foam washed with methanol.

complex viscosity (η^*) of the mixture at the gelation time (t_{gel}), ranging from 63000 Pa s to 610 Pa s, respectively (Figure 2c). Therefore, the rheological results show a direct relationship between the foaming behaviour, the stability of the foam and the η^* variation during reactive foaming. At the optimized ratio of BC6/PETMP of 1/0.25 (or BC6/C5 = 1/1) where $\eta^* \approx 11000$ Pa s (at $t_{gel} \approx 640$ s) within the upper and lower viscosity the foamability and stability were enhanced. The complexity of the foaming process is further highlighted by the fact that inadequate viscous strength of larger-sized cells becomes more pronounced at higher BC6 contents, and the associated relative drop in storage modulus (G') increases (see Figure S8 for further discussion).

Exploiting the great structural and functional versatility of polyols to afford rigid, semirigid, or flexible PU foams is a generic principle for tuning the mechanical property space of PU materials. For instance, flexible foams are made of polyols with longer alkyl chains and low functionality, while rigid PU foams are based on polyols of high functionality and shorter chains, because of the higher degree of cross-linking. Based on this, we added a polyol to our reactive formulation to increase control over the foaming process, which would be expected to have a decisive influence on achieving structural control over the PC foams.

As depicted in Figure 2a, the preparation strategy of the self-blown foams is to combine the reactive formulation containing BC6, C5, and PETMP with a polyol, polycaprolactone triol (PCL–T) as a hydroxyl initiator to encourage the polymer chain growth and cross-linking, as well as to expand the range of mechanical properties. We worked under a fixed [BC6]/[PCL–T]/[PETMP] = 1/1/0.25 and [C5]/[PETMP] = 1/0.25; thus, 14 % and 86 % of the overall hydroxyl groups are from PCL–T and the poly(hydroxythioether), respectively.

The mixture was homogenized in PTFE beakers for 10 minutes at 70 °C, and foaming was then achieved at 70 °C for 1 hour by adding DBU (5 mol%) to the formulation.

As can be seen in Figure 2c, the optimized formulation allowed for the preparation of open-cell flexible foams with good shape and structure. Detailed kinetic investigations of the PC foaming process were performed by in situ ATR-IR spectroscopy at 70 °C. (Figure 2b). The consumption of C5 was followed by the decrease of the peak at around 1800 cm^{-1} (C=O stretch of C5's carbonate group). The evolution of the single intense vibrational frequency of C=O

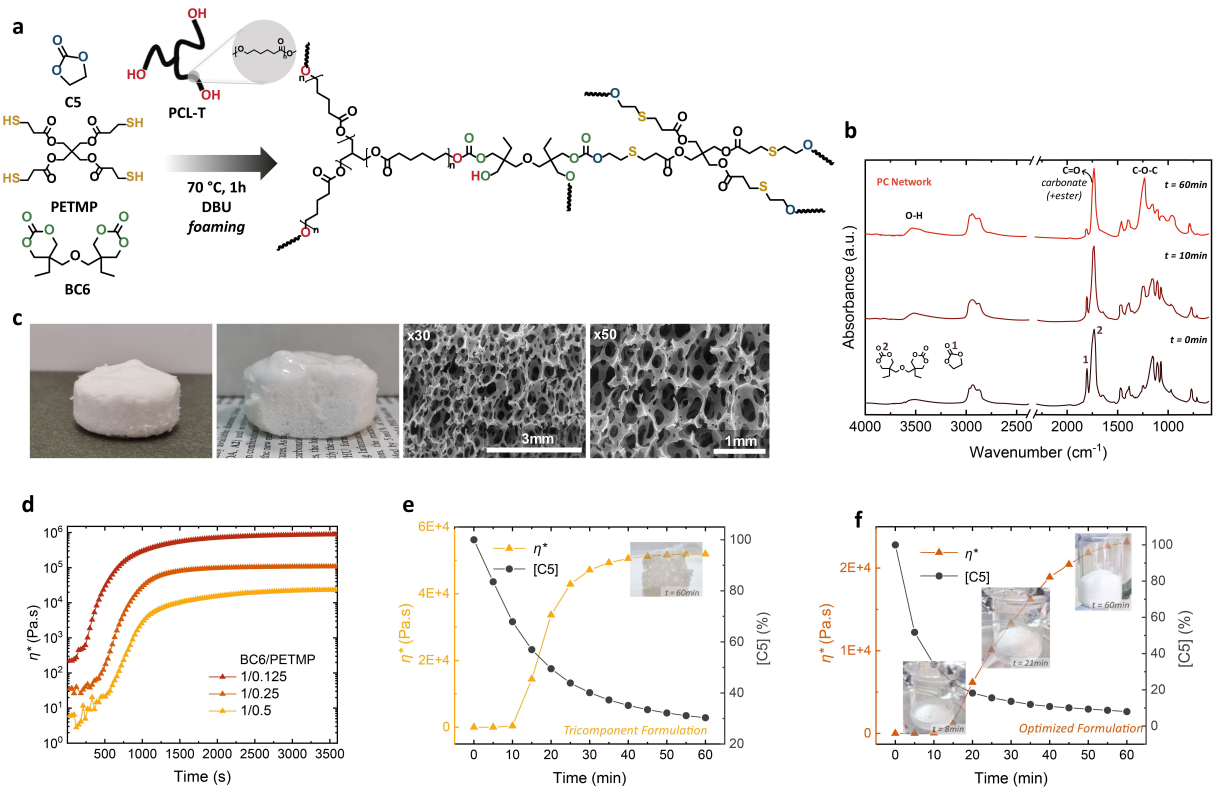

Figure 2. (a) Components of the optimized formulation and Scheme for producing the self-blown PC foams. Conditions: [BC6]/[C5]/[PETMP] = 1/1/0.25 and [BC6]/[PCL–T]/[PETMP] = 1/0.167/0.25, DBU (5 mol% compared to cyclic carbonates), homogeneously mixed (approx. 10 min) and cured at 70 °C for 1 h. (b) In situ ATR-IR spectroscopy monitoring the PC foaming process. (c) SEM images of the self-blown PC foam made from a polyester polyol (PCL–T). (d) In situ measurements of complex viscosity (η^*) development during reactive foaming at 70 °C for various molar concentration of PETMP: 0.125, 0.25 and 0.5. (e), (f) Change of complex viscosity (η^*) and 5CC concentration over time. The η^* was determined through oscillatory time sweep. (e) Inset: A single image capturing the foam prepared using a tricomponent (unoptimized) formulation, highlighting its distinctive reticulated structure. (f) Inset: The captured images at 8, 21, and 60 minutes during foam formation demonstrate a clear correlation between the rise of the foam and the corresponding increase in viscosity.

groups–esters and cyclic/linear carbonates–at around 1734 cm^{-1} suggested a complex absorption band consisting of overlapping bands. Nevertheless, a new peak at 1234 cm^{-1} emerged, which was attributed to the conversion of the C–O–C group from BC6 to a linear polycarbonate.

To better understand the underlying principles of this new foaming process, we attempted to relate the foaming reaction kinetics (e.g., the degree of conversion of 5CC) to the rheological parameters of the reactive system (e.g., complex viscosity (η^*)). To be able to perform this analysis, we compared the optimized composition including PCL–T as our reference system with the tricomponent (unoptimized) formulation with a ratio of [BC6]/[PCL–T]/[PETMP] of 1/1/0.25. Figure 2e,f was then plotted through a combination of the degree of conversion of 5CC and variation of complex viscosity (η^*) as a function of time (see Figure S9 for the graph of 2nd derivative of η^* vs. *time*).

Figure 2e, where the inset is a representative photograph of the resulting foam suggests that the viscosity of the tricomponent formulation only reached up to 162 Pa s as the gelation started ($t_{gel} \approx 840$ s) at around 80 % of conversion of C5. On the other hand, the optimized formulation differed by up to 10-fold in viscosity ($\eta^* \approx 2800$ Pa s) at its $t_{gel} \approx 720$ s when less than half of C5 was decarboxylated (Figure 2f; see also the inset). This allowed a distinct improvement in the foamability and foam stability, which is reflected by the foam morphology, such as a more uniform cell structure with less deformed cells (Figure 2c) and mechanical properties, such as enhanced dimensional stability and rigidity, which will be discussed further in detail later.

The thermal properties of the foam were analyzed by differential scanning calorimetry (DSC) and thermogravimetric analyses (TGA) and are summarized in Table 1.

The glass transition temperature (T_g) was −14 °C. The degradation temperature ($T_{d5\%}$) at around 115 °C showed a low-temperature degradation profile in comparison with other similar systems (Figure S10).

We attribute this to the presence of residual DBU, which may promote PC foam shrinkage and de-crosslinking at higher temperatures. After washing the PC foam with methanol, the $T_{d5\%}$ of the foam increased considerably from 115 °C to 222 °C, supporting this assumption (Figure S11).

Role of Additives in Enhancing Morphology and Mechanical Properties

In the case of the PCL-based reference formulation, cell rupture and coalescence occurred during the period rapid cell growth. As a result, the PC foam showed no well-defined open-cell structure but numerous interconnected cells. As reported in the literature, the cell structure can be controlled by additives to improve the physical-mechanical properties. The logic of selection of surface-functionalized nanoparticles as additives is to promote chemical or physical bonding with the foam matrix when uniformly dispersed and thereby, unique nucleating effects.[18] Laponite, for instance, is a hydrophilic nanosheet clay that acts as a reinforcing filler but has also been proposed to serve as a nucleating agent to favor homogeneous nucleation, leading to a smaller cell size.[10] Alternatively, di-trimethylolpropane (di-TMP), which possesses reactive hydroxyl groups, can also be used to increase the degree of crosslinking as well as the length of the hard segment and thus acts as a chain extender and curing agent, enabling higher viscosity prior to foaming.

Morpho-structural properties of the self-blown PC foams, including the cells size and distribution, as well as the ratio of opened and closed cells were analyzed by scanning electron microscopy (SEM, Figure 3 and Figure S12) and their characteristics are summarized in Table 1. The morpho-structural properties of the self-blown PC foam were substantially modified upon the addition of these additives. As observed in the SEM images in Figure 3a,b open-cell microcellular foams with near-spherical cell shapes, and circular holes between the faces (as depicted in Fitzgerald's work[19]) were formed. The open porosity of the foams was then evaluated by the holes-on-cell area ratio A_h/A_c and are reported in Table 1.

The PC foam loaded with Di-TMP displayed a large average cell diameter of 0.98 ± 0.37 mm and the addition of Laponite further reduced the cell size to 0.70 ± 0.29 mm. Holes-on-cell area ratios A_h/A_c were in the same range with 9.1 % and 10.6 % for Di-TMP and Laponite, respectively. Nevertheless, the foam density

strongly increased from 0.180 $g\,cm^{-3}$ (None) and 0.200 $g\,cm^{-3}$ (Laponite) to 0.278 $g\,cm^{-3}$ (Di-TMP). All foams had a T_g falling within a range of −15 ± 1 °C. This can be attributed to the formulation comonomers which are similar for all these foams. Additionally, no significant changes in the degradation profiles were observed for the foams with additives ($T_{d5\%} \approx 120$ °C).

The changes to the cellular morphology and density by incorporating additives also resulted in significant changes in the mechanical properties of the foams. Table S2 summarizes the values of the mechanical properties, including compressive stress (σ) at 50 % strain (ε) and shape recovery (R_r). As shown in Figure 4b, adding Laponite or Di-TMP to the formulation led to substantial strengthening, and these reinforced foams reached higher σ of 28 ± 4 and 75 ± 6 kPa, respectively. On the other hand, the PC foam containing neither Laponite nor Di-TMP exhibited a relatively low σ of 14 ± 3 kPa at 50 % strain. It should be noted that a higher foam density presents a higher compressive strength, and therefore for all formulations, the compressive strength

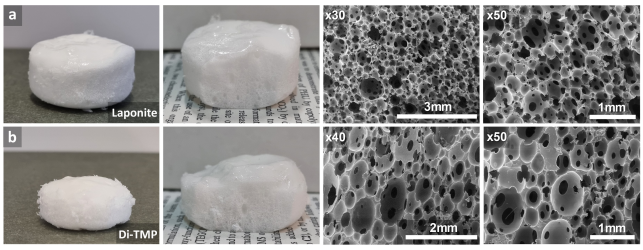

Figure 3. SEM characterizations of self-blown PC foams. (a) PC foam loaded with 1.5 wt% Laponite. (b) PC foam loaded with 0.125 equiv. Di-TMP compared to BC6.

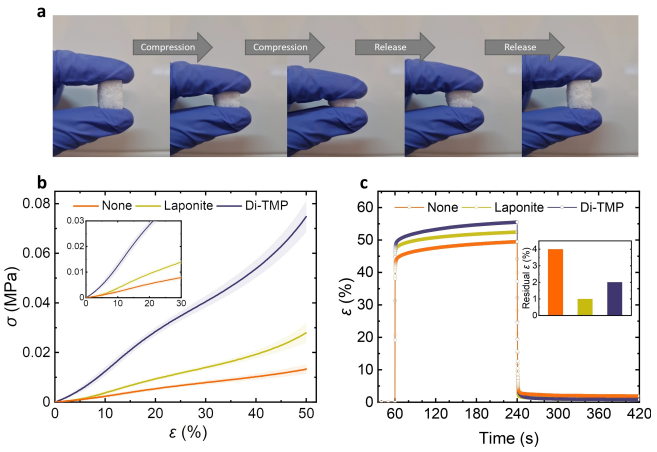

Figure 4. (a) The compression-recovery showing that the additive-free PC foam recovers its original shape after compression by more than 90%. b) Compression tests of the PC foams with or without additives. The standard deviation of each curve is represented as its own colored shadow. Inset: A close-up zoom of the elastic region, illustrating the significant increase in modulus achieved through the addition of Di-TMP (c) Creep profiles of the self-blown PC foams. Inset: The accumulated residual strain (ε) levels observed during the creep test.

appears to be principally dependent upon the resulting foam density (Figure S13).

As shown in Figure 4a, the self-blown PC foams exhibit excellent compressibility, flexibility, and recoverability. For example, the PC foam can be compressed by more than 90 %, and completely recover its original shape without mechanical failure. In order to assess the ability of the foams to recover their original shape after compression, creep tests were conducted. The creep profiles of the foams are shown in Figure 4c. During a constant stress applied for 3 minutes, the foams experienced a rapid increase in strain (ε), reaching a range of 49 % to 55 %. Upon stress release, the ε promptly decreased, leaving behind a small residual ε (<4 %). Notably, the foams loaded with additives exhibited residual ε levels below 2 %, resulting in enhanced shape recovery (R_r) ≈ 99 %.

The observed differences in mechanical performance can be correlated to the morphological properties of the foams, which can be tuned by the rational selection of additives. Indeed, the lower creep behavior of the additive-loaded foams can be attributed to their reduced porosity and more closed-cell structure, which restricts gas diffusion. Additionally, the presence of smaller cells with thicker cell walls improves compressive stress and facilitates viscoelastic recovery.

Recycling Methods and Prospects

Cross-linking of polymer chains makes recycling of many foams challenging and narrows their end-of-life options to incineration or landfill.[20] Moreover, the current physical recycling methods are insufficient to manage the substantial volumes of foam waste generated.[21] Developing recycling strategies for cross-linked polymeric materials is therefore crucial to manage the significant accumulation of waste. To tackle this issue, the introduction of dynamic cross-links into polymer networks has emerged as a promising solution, as it can potentially enable the reprocessing of thermoset-like materials.[22]

The chemistry of carbonates is similar to that of esters. Unfoamed PC thermosets capable of recycling were recently reported by transcarbonation exchange reactions with free hydroxyl groups, which were induced at elevated temperatures in the presence of a Ti-based catalyst.[12c] Herein, the dynamic nature of our thermoset foams is demonstrated by foam-to-film reprocessing. The self-blown PC foams also contain many pendant hydroxy groups (Figure 5a), and thereby transcarbonation, as well as transesterification reactions, are expected to allow reprocessing of the foams into recycled materials.

For the proof-of-concept, we evaluated the circularity of our PC foam by reprocessing to bulk, intact PC films via compression molding at 90 °C for 15 min under ≈3 MPa of pressure (Figure 5a). The additive-free foam yielded a transparent homogeneous film, as shown in SEM images before and after reprocessing in Figure 5a (see Supporting Information for further discussion). DMTA was used to measure the thermomechanical properties of the reprocessed film (Figure 5b). The storage modulus of the reprocessed film shows a rubbery plateau above the T_g, suggesting the preservation of its cross-linked nature after reprocessing. The structural homogeneity of the resulting film is further confirmed by a single, narrow T_g. Figure S14 shows the FTIR specta of the PC foam and the reprocessed film, confirming no structural transformations of the polymer occured during reprocessing.

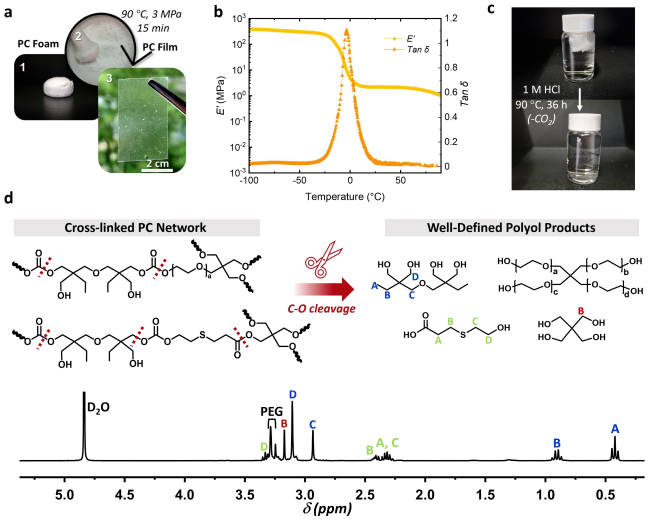

Figure 5. (a) Demonstration of the foam reprocessability by hot pressing at 90 °C for 15 min. A homogeneous film was obtained (thickness = 0.3 mm, scale bar = 2 cm). (b) Temperature variation of the storage modulus (E'), and *tan δ* plots for the reprocessed film. (c) Degradation of the foam based on 4-arm PEG via hydrolysis in the acidic environment (1 M HCl), yielding CO_2 and hydroxy-terminated monomers at 90 °C for 36 h. (d) Scheme and ^{1}H NMR of the hydrolytic degradation products.

Nevertheless, a slightly higher T_g value of −3 °C is attributed to an increase in cross-linking density during reprocessing, an effect that can be observed in the gel fractions of the PC foam and the corresponding reprocessed film, which were measured as 83 % and 87 %, respectively. In addition to the mechanical recycling route outlined above, we examined the end-of-life management of our foams using chemical recycling. In order to avoid the hydrolysis of the ester groups of PCL–T, we first prepared the foam based on pentaerythritol ethoxylate (4-arm PEG) including no degradable bonds. This foam was hydrolyzed by acid (1 M HCl, 90 °C, 36 h) similar to Dichtel's work[12c] on PC network depolymerization, resulting in a homogeneous solution (Figure 5c). The formation of the related alcohol species and the absence of carbonyl functional groups suggests a preferred degradation pathway, including the hydrolysis of the ester/carbonate bonds followed by decarboxylation. The structure of these alcohol monomers was elucidated by ^{1}H NMR and ^{13}C NMR spectroscopies of the degradation products (Figure 5d and Figure S16). The formation of the expected di(trimethylolpropane) (di-TMP) was identified by the typical signals for the two neighboring alkyl groups $-CH_2\underline{CH_3}$ and $-\underline{CH_2}CH_3$ at 0.39–0.45 ppm and 0.87–0.94 ppm, as well as the methylene protons bound to etheric oxygen and alcoholic OH at 2.93 ppm and 3.10 ppm, respectively. The ^{13}C NMR spectrum showed one resonance ($\delta = 176$ ppm) of a carbonyl moiety corresponding to the carboxylic acid and no other observable carbonyl resonance, which underscores the completeness of degradation. All these assignments for proposed structures were confirmed by HSQC and HMBC analyses (Figure S17 and S18).

Conclusion

In this work, the first strategy for the synthesis of microcellular self-blown polycarbonate foams has been reported. The synthetic process makes use of the distinct reactivity of thiols and alcohols in the ring opening of different sized cyclic carbonates. Central to this strategy is the hydroxyl functionality provided by the decarboxylative S-alkylation of a thiol, which can trigger a cascade process. This involves the generation of carbon dioxide, CO_2, and a subsequent ring opening of the 6-membered cyclic carbonate, resulting in polycarbonate network formation in the absence of an external alcoholic initiator.

PC foaming was then considered from reactive formulations containing a bis(6-membered cyclic carbonate), a polyol, and a tetrafunctional thiol. In the presence of DBU, this one-pot process was successful using mild conditions (70 °C for 1 h). The developed formulations enable the production of highly flexible foams with open-cell. Through the use of additives such as Laponite clay and Di-TMP, the production of highly flexible foams with open-cell, widely tunable morphologies were shown to be possible.

Overall, the strategy shows the potential for a cradle-to-cradle lifecycle as the cross-linked foams can be reprocessed into films or degraded by facile hydrolysis. This new conceptual approach toward more sustainable foaming processes for producing alternative foam materials composed of a recyclable and eco-friendly polymer opens up a range of interesting possibilities with potential yet to be discovered.

Acknowledgements

Anton Paar is acknowledged for the loan of the MCR702 rheometer, Paolo Edera and Imed Ben Tarcha are thanked for help in rheological measurements. The research leading to these results has received funding from the VITRIMAT program of the European Union's Horizon 2020 research and innovation programme under the Marie Sklodowska-Curie Grant agreement No 860911.

Conflict of Interest

The authors declare no conflict of interest.

Data Availability Statement

The data that support the findings of this study are available from the corresponding author upon reasonable request.

Keywords: CO_2 · Cyclic Carbonates · Foams · Polycarbonates · Thiols

[1] a) J. Li, W.-Y. Wong, X. Tao, *Nanoscale* **2020**, *12*, 1281–1306; b) N. V. Gama, A. Ferreira, A. Barros-Timmons, *Materials* **2018**, *11*, 1841.
[2] S.-T. Lee, N. S. Ramesh, *Polymeric Foams: Mechanisms and Materials*, CRC, Boca Raton, **2004**, p. 12.
[3] a) G. Coste, C. Negrell, S. Caillol, *Eur. Polym. J.* **2020**, *140*, 110029; b) F. Monie, T. Vidil, B. Grignard, H. Cramail, C. Detrembleur, *Mater. Sci. Eng. R* **2021**, *145*, 100628.
[4] S.-T. Lee, D. P. K. Scholz, *Polymeric Foams: Technology and Developments in Regulation*, *Process*, *and Products*, CRC, Boca Raton, **2008**, pp. 1–20.
[5] F.-L. Jin, M. Zhao, M. Park, S.-J. Park, *Polymer* **2019**, *11*, 953.
[6] https://www.smithers.com/services/market-reports/materials/the-future-of-polymer-foams-to-2025 (accessed April 2022).
[7] H.-W. Engels, H.-G. Pirkl, R. Albers, R. W. Albach, J. Krause, A. Hoffmann, H. Casselmann, J. Dormish, *Angew. Chem. Int. Ed.* **2013**, *52*, 9422–9441.
[8] R. J. Ouellette, J. D. Rawn, *Organic Chemistry: Structure*, *Mechanism*, *Synthesis*, Academic Press, New York, **2018**, p. 820.
[9] A. Cornille, S. Dworakowska, D. Bogdal, B. Boutevin, S. Caillol, *Eur. Polym. J.* **2015**, *66*, 129–138.
[10] F. Monie, B. Grignard, J.-M. Thomassin, R. Mereau, T. Tassaing, C. Jerome, C. Detrembleur, *Angew. Chem. Int. Ed.* **2020**, *59*, 17033–17041.
[11] a) J. Xu, E. Feng, J. Song, *J. Appl. Polym. Sci.* **2014**, *131*, 39822; b) Y. Yu, B. Gao, Y. Liu, X.-B. Lu, *Angew. Chem. Int. Ed.* **2022**, *61*, e202204492.
[12] a) Y. Liu, X.-B. Lu, *J. Polym. Sci.* **2022**, *60*, 3256–3268; b) J. Huang, J. C. Worch, A. P. Dove, O. Coulembier, *ChemSusChem* **2020**, *13*, 469–487; c) R. L. Snyder, D. J. Fortman, G. X.

De Hoe, M. A. Hillmyer, W. R. Dichtel, *Macromolecules* **2018**, *51*, 389–397; d) M. Taherimehr, P. P. Pescarmona, *J. Appl. Polym. Sci.* **2014**, *131*, 41141; e) T. Artham, M. Doble, *Macromol. Biosci.* **2008**, *8*, 14–24.

[13] a) T. Şucu, M. P. Shaver, *Polym. Chem.* **2020**, *11*, 6397–6412; b) C. D. Roland, C. M. Moore, J. H. Leal, T. A. Semelsberger, C. Snyder, J. Kostal, A. D. Sutton, *ACS Appl. Polym. Mater.* **2021**, *3*, 730–736.

[14] a) W. Yu, E. Maynard, V. Chiaradia, M. C. Arno, A. P. Dove, *Chem. Rev.* **2021**, *121*, 10865–10907; b) K. Saito, C. Jehanno, L. Meabe, J. L. Olmedo-Martínez, D. Mecerreyes, K. Fukushima, H. Sardon, *J. Mater. Chem. A* **2020**, *8*, 13921–13926; c) M. Scharfenberg, J. Hilf, H. Frey, *Adv. Funct. Mater.* **2018**, *28*, 1704302.

[15] a) N. Weingart, D. Raps, J. Kuhnigk, A. Klein, V. Altstädt, *Polymer* **2020**, *12*, 2314; b) D. Jahani, A. Ameli, M. Saniei, W. Ding, C. B. Park, H. E. Naguib, *Macromol. Mater. Eng.* **2015**, *300*, 48–56; c) A. K. Bledzki, H. Kirschling, M. Rohleder, A. Chate, *J. Cell. Plast.* **2012**, *48*, 301–340; d) J. W. S. Lee, K. Wang, C. B. Park, *Ind. Eng. Chem. Res.* **2005**, *44*, 92–99; e) R. Gendron, L. E. Daigneault, *Polym. Eng. Sci.* **2003**, *43*, 1361–1377; f) D. G. LeGrand, J. T. Bendler, *Handbook of Polycarbonate Science and Technology*, Marcel Dekker, New York, **2000**, p. 313; g) V. Kumar, J. Weller, *J. Eng. Ind.* **1994**, *116*, 413–420.

[16] M. M. Bernal, M. A. Lopez-Manchado, R. Verdejo, *Macromol. Chem. Phys.* **2011**, *212*, 971–979.

[17] H. Al-Moameri, Y. Zhao, R. Ghoreishi, G. J. Suppes, *Ind. Eng. Chem. Res.* **2016**, *55*, 2336–2344.

[18] B. Merillas, F. Villafañe, M. Á. Rodríguez-Pérez, *Polymer* **2021**, *13*, 2952.

[19] C. Fitzgerald, I. Lyn, N. J. Mills, *J. Cell. Plast.* **2004**, *40*, 89–110.

[20] A. Kemona, M. Piotrowska, *Polymer* **2020**, *12*, 1752.

[21] a) T. Vanbergen, I. Verlent, J. De Geeter, B. Haelterman, L. Claes, D. De Vos, *ChemSusChem* **2020**, *13*, 3835–3843; b) I. A. Ignatyev, W. Thielemans, B. Vander Beke, *ChemSusChem* **2014**, *7*, 1579–1593.

[22] a) N. Zheng, Y. Xu, Q. Zhao, T. Xie, *Chem. Rev.* **2021**, *121*, 1716–1745; b) J. M. Winne, L. Leibler, F. E. D. Prez, *Polym. Chem.* **2019**, *10*, 6091–6108; c) D. J. Fortman, J. P. Brutman, G. X. De Hoe, R. L. Snyder, W. R. Dichtel, M. A. Hillmyer, *ACS Sustainable Chem. Eng.* **2018**, *6*, 11145–11159; d) W. Denissen, J. M. Winne, F. E. D. Prez, *Chem. Sci.* **2015**, *7*, 30–38.

Manuscript received: June 13, 2023
Accepted manuscript online: August 20, 2023
Version of record online: September 19, 2023